Humidity Required for Ice Nucleation from the Vapor onto Silver Iodide and Lead Iodide Aerosols over the Temperature Range −6 to −67°C

ANDREW G. DETWILER AND BERNARD VONNEGUT

State University of New York at Albany, Albany, NY 12222

(Manuscript received 9 January 1981, in final form 15 May 1981)

ABSTRACT

The ice saturation ratio at which 1% of aged silver iodide and lead iodide aerosol particles nucleate ice from moist air is observed to depend on temperature. Between roughly −30 and −67°C the threshold for both aerosol types rises slowly with decreasing temperature in agreement with a simple classical nucleation theory. Between −6 and −30°C the threshold for the silver iodide aerosol rises more rapidly than predicted by simple theory while the threshold for lead iodide decreases.

1. Introduction

Extensive layers of the troposphere often become supersaturated with respect to ice but remain visibly cloudless. Even ice particle clouds do not generally form until humidities approach saturation with respect to liquid water (Heymsfield, 1975). Such clear ice-supersaturated regions can be intentionally seeded with ice nucleating agents in order to produce widespread cirrus cloudiness. Successful preliminary experiments have been carried out with both dry ice (Schaefer, 1950; Jayaweera and Ohtake, 1972) and silver iodide (Vonnegut and Maynard, 1952).

Such artificially produced clouds are of practical importance, for they have the potential of moderating surface diurnal temperature extremes (Nicodemus and McQuigg, 1969) and perhaps altering the location and/or intensity of convective cloud systems (Gray and Jacobson, 1977; Gannon, 1978).

In order to evaluate and design techniques for artificially influencing ice formation in clear air and in order to improve our understanding of the formation of natural cirrus, it is necessary to have a much better understanding of the ice nucleation process than is presently available. Although extensive studies have been carried out on natural and artificial ice nucleation at temperatures in the range 0 to −30°C, little or no experimental data are available at the much lower temperatures where the deepest and most extensive regions of air supersaturated with respect to ice generally occur. In order to achieve a better understanding of heterogeneous nucleation processes and to secure quantitative information concerning the activity of ice nucleating aerosols in clear air, experiments were carried out on the activity of silver iodide and lead iodide aerosols at various supersaturations down to temperatures as low as −67°C.

2. Theoretical background

The classical theory of nucleation provides some background for understanding measurements of heterogeneous ice nucleation. Following Fletcher (1969a), the nucleation rate equation can be written as

$$J = Kr^2 \exp\left(-\frac{\Delta F^*}{kT}\right). \tag{1}$$

In this expression, J is the nucleation rate on a particle surface, i.e., number of ice germs nucleated on a particle of radius r per unit time. K is a kinetic factor which represents the rate at which molecules become available to growing ice embryos on the particle surface both from the vapor directly and also by surface diffusion of adsorbed water molecules. It also can be thought to contain a factor specifying what fraction of the particle surface area is covered by active nucleating sites and something about the characteristics of these sites. The factor r^2 is proportional to the total particle surface area. In the argument of the exponential function, k is Boltzmann's constant, T is temperature on the absolute scale, and ΔF^* is the free energy of formation of the critical ice germ at an active site on the particle surface.

If one considers only the addition of molecules directly from the vapor, the kinetic factor K decreases with decreasing temperature for a given ice saturation ratio. This is due to smaller molecular velocities, a decrease in the size of the critical ice

0021-8952/81/091006-07$05.75

germ, and also to lower vapor densities corresponding to a given saturation ratio at lower temperatures. On average, the addition of water molecules to an embryonic cluster by surface diffusion also decreases as temperature decreases (Lamb and Scott, 1974) and will contribute to a decrease in K, also.

However, temperature dependence in the argument of the exponential function dominates the variation of nucleation rate with temperature for observable nucleation rates. The standard classical expression for this argument is given, following Dufour and Defay (1963) and Fletcher (1969b), as

$$\frac{\Delta F^*}{kT} = \frac{16\pi\sigma^3 V^2 N f(m, x)}{3R^3T^3 \ln^2 S}. \quad (2)$$

The embryo is approximated as spherical. The surface free energy of the ice-air interface is represented as σ; V is the molar volume of water in the ice phase, R the universal gas constant, S the ice saturation ratio, N the number of molecules in a mole of a substance, and $f(m, x)$ a function which represents the geometrical and surface-chemical compatibility of the nucleating particle surface and the ice embryo, where m is the cosine of the angle of contact between ice and the particle and x the ratio of the equivalent spherical radius of the particle to that of the ice germ. The germ radius itself is a function of T, S and σ.

Within this expression, σ, V and $f(m, x)$ are functions of temperature, and T^3 appears explicitly in the denominator. Considering only the explicit T^{-3} temperature dependence in the argument of the exponential in (1), it is apparent that if the right-hand side of (1) is to be held constant as T decreases, then S must increase to compensate for it, in the proportion

$$\frac{\ln^2 S_{T1}}{\ln^2 S_{T0}} = \frac{T_0^3}{T_1^3}$$

$$S_{T1} = S_{T0}^{(T_0/T_1)^{3/2}}. \quad (3)$$

For example, if S_{T0} is 1.15, T_0 is 258 K (−15°C) and T_1 is 213 K (−60°C), then this relation predicts that S_{T1} will be 1.20. For S_{T0} closer to 1.0 the proportional increase in S_{T1} with decreasing T_1 is less than this; for $S_{T0} > 1.15$, the proportional increase in S_{T1} with decreasing T_1 is greater.

It turns out that the corresponding change in the kinetic term over this same temperature range, considering only addition of molecules from the vapor to the growing ice cluster, would require an increase in S by ~1% to compensate for the decreasing temperature if K is required to be held constant.

The temperature dependences of some of the other parameters are not accurately known. In fact, nucleation experiments offer one method for deriving such information. Observations indicate that the temperature dependences of σ and V are probably very weak (Pruppacher and Klett, 1978). For particles an order of magnitude or more larger than the size of an ice germ at a given temperature and ice saturation ratio, the temperature dependence of $f(m, x)$ also is probably very weak (Fletcher, 1958).

The nucleation rate can be observed directly when particles in an aerosol nucleate ice. Let us define the threshold ice saturation ratio as the lowest ice saturation ratio at a given temperature at which, say, 1% of the aerosol particles nucleate ice crystals within a certain time period. If the particle size distribution is held constant, then Eq. (3) predicts that the threshold ice saturation ratio must slowly rise as temperature falls in order to maintain a constant nucleation rate if other factors are held constant.

In contrast, the available observations suggest that many aerosols have a nearly constant, temperature-independent, threshold ice saturation ratio below a temperature where the threshold corresponds to a humidity somewhat less than liquid phase saturation (Mason and van den Heuvel, 1959; Schaller and Fukuta, 1979). These observations only extend down to about −30°C, however.

In order to investigate further the extent of agreement between observation and theory, two series of ice nucleation observations over the temperature range −6 to −67°C were made. The ice nucleating activity of silver iodide and lead iodide aerosols generated from a heated, coated wire was investigated over this range of temperatures.

3. Experimental apparatus and procedure

Ice nucleation from the vapor onto silver iodide and lead iodide aerosols was observed in a standard parallel-plate thermal-gradient diffusion chamber. The procedures followed were broadly similar to those of Mason and Hallett (1956), Mason and van den Heuvel (1959), and Schaller and Fukuta (1979). Important aspects of these procedures are summarized in this section, while detail is given in Detwiler (1980).

a. Aerosol generation

In order to produce an aerosol, we coated a small stainless steel wire coil with silver iodide or lead iodide and then heated the coil electrically. This led to aerosol formation in the air near the coil.

Aerosol was generated in an aluminum vessel, roughly 2×10^4 cm^3 capacity, that was placed in a laboratory cold chamber (see Fig. 1). It was connected via 0.5 cm ID copper tubing to the thermal-gradient diffusion chamber. Similar copper tubing led from the diffusion chamber out through a port

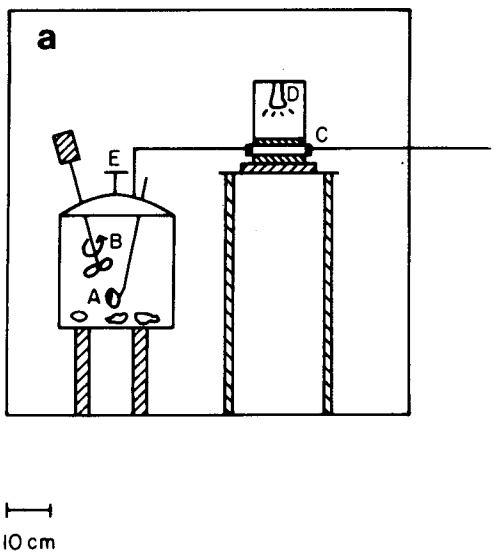

FIG. 1a. The experimental apparatus. A is the wire coil, B an 8 cm plastic propeller, C the thermal gradient diffusion chamber, D a 40 W incandesent light bulb inside an inverted 13 cm diameter metal can, and E an absolute filter that removes particles from air entering the storage vessel from the cold chamber to replace the sample air drawn through the diffusion chamber and out through the CN counter. The apparatus is shown set up in the 1 m^3 cold chamber. The cold chamber fans circulate air around all sides of the storage vessel and underneath the diffusion chamber platform.

in the cold chamber to a Gardner condensation nucleus counter (Gardner Associates, Schenectady, New York). A large seven-plane plexiglass window in the side of the cold chamber allowed the apparatus to be viewed. The volume between the plates of the diffusion chamber was illuminated by a 0.95 mW He-Ne laser which was outside the cold chamber. The 0.3 cm diameter laser beam was reflected off of a mirror behind the diffusion chamber and then through the diffusion chamber so that the particles inside the chamber could be viewed from outside by light scattered roughly in a direction 135° from the entering laser beam. Viewing was done through a low-power telescope, from outside the cold chamber. The volume of the beam observed was roughly 0.1 cm^3.

Silver iodide was applied to the wire coils either in a solution with hydriodic acid in acetone or as a few milligram chunk of pyrotechnic flare material which was slightly moistened with water to aid adhesion. The flare material used was the LW-83 formulation, which is a predecessor of the fairly common TB-1 formulation used today (St. Amand *et al.*, 1970). Lead iodide was applied as a thick water paste. Reagent-grade materials were used for both the silver iodide solution and the lead iodide paste.

Separate coils were used for each type of coating. They were formed by winding 0.02 cm diameter wire tightly about a 0.3 cm diameter cylinder. A coil was cleaned prior to application of the coating by passing an electrical current through it and heating to a bright red color in room air for several minutes. The coil was dried after the coating was applied and then inserted, on a glass rod, into the aerosol storage vessel. The entire cold chamber was then cooled to some subfreezing temperature at which the experiment was to be performed. Silica gel was used to keep the humidity in the aerosol storage vessel beneath ice saturation (Higuchi and Fukuta, 1966).

The coil was heated electrically to bright red heat as a fan blew air over it. This led to the creation of an aerosol consisting of condensed particles formed from the volatilized coating and formed also from substances derived from the wire itself and perhaps also from environmental gases in the hot air near the wire (Vonnegut, 1953; O'Connor *et al.*, 1959; O'Connor and Roddy, 1966). The aerosol generation technique was the same at all temperatures in both the silver iodide and lead iodide series. Therefore, it is highly probable that the aerosols had the same composition at all temperatures.

The aerosol was aged for several hours at the cold chamber temperature. The hand pump connected to the Gardner counter was used to draw aerosol from the storage vessel through the diffusion chamber, where its ice nucleating ability could be tested at various ice saturation ratios and tempera-

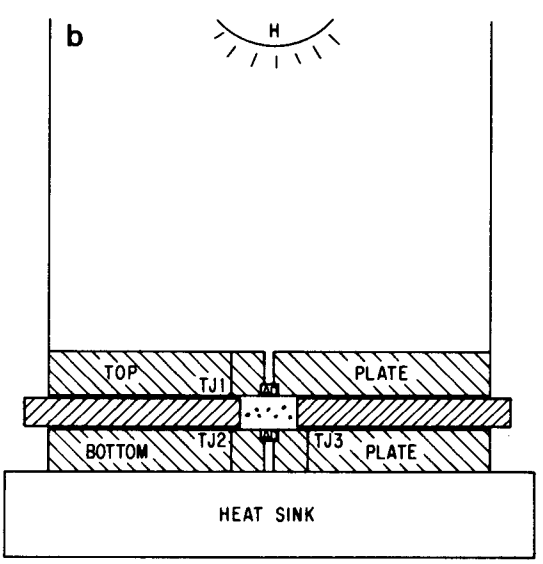

FIG. 1b. Detail of the diffusion chamber. TJ1 and TJ2 are copper-constantan junctions used to measure the vertical temperature gradient across the chamber. TJ3 is a similar junction forming a couple with another junction in an ice-water mixture and is used to determine the bottom-plate temperature. The AD sensors are semiconductor temperature sensors and are also used to measure the diffusion chamber vertical temperature gradient. Foam rubber insulation surrounds the plastic ring separating the aluminum plates, except where flat clear windows are set to allow lighting and viewing the chamber interior. Ice particles are depicted as they might appear to the experimenter in the laser beam.

tures. The bottom plate of the diffusion chamber was at the temperature of the cold chamber (and, therefore, the stored aerosol), and the top plate was heated from above by an incandescent light bulb.

Aerosol concentrations in the storage vessel and diffusion chamber could not be determined directly during our experiment. When aerosol was drawn out of the experimental apparatus during our experiments and through the Gardner counter, large losses occurred due to the temperature gradients in the tubing where it left the cold chamber. Therefore a series of tests was done with the experimental apparatus at room temperature in which measurements of the aerosol particle concentration in the 2×10^4 cm^3 aluminum storage vessel were made for a period of time following initial aerosol generation. One or two minutes after generation, condensation nucleus concentrations determined by the Gardner counter were on the order of 10^6 cm^{-3}. After 2 h or so concentrations were on the order of 10^4 cm^{-3} and decayed very slowly with further aging. Even after 24 h concentrations had decayed to only around 10^3 cm^{-3}, typically.

Tests with an electrical aerosol analyzer (TSI, Inc., St. Paul, Minnesota) showed the same trend of decreasing particle concentration over the first few hours. The concentration of condensation nuclei counted with the Gardner was, to within 10%, the same as the concentration of particles counted with the electrical aerosol analyzer.

The aerosol concentration decay curve measured at room temperature was assumed valid at all temperatures and for all trials reported here. In particular, it was assumed that after 2 or 3 h, the aerosol particle concentration in the storage vessel was about 10^4 cm^{-3} and that this same concentration of particles was drawn from the storage vessel through the diffusion chamber where nucleation was observed.

Ice particle concentration in the diffusion chamber was judged by counting ice particles within the known volume of the laser beam. Relative humidity and ice saturation ratio were calculated from the measured temperatures of the ice-covered diffusion chamber plates using the Goff-Gratch formulas (Letestu, 1966).

b. Aerosol particle sizes

Although the particles generated from a ventilated hot wire can be initially smaller than 10^{-2} μm in diameter, coagulation rapidly produces much larger particles unless rapid dilution occurs. After the aerosol has aged, small particles $\ll 0.1$ μm diameter or so will be lost due to coagulation and attachment to container walls. Particles $\gg 1.0$ μm diameter will fall to the bottom of the relatively small container used here for aerosol storage in a relatively short period of time (tens of minutes). Thus particles on the order of 0.1 μm diameter will dominate the size distribution after storage for several hours.

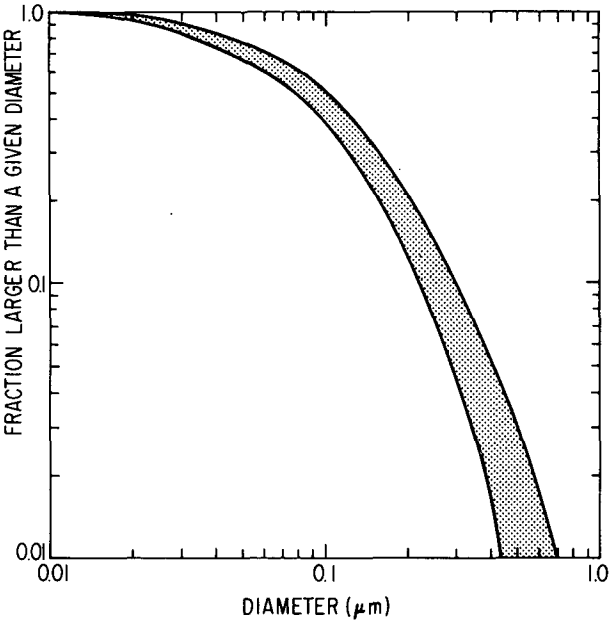

FIG. 2. The range of cumulative aerosol particle size distributions observed for aged silver iodide aerosols. All aerosols were several hours old and aged in a metal storage vessel at room temperature.

As an example, measurements of the aerosol particle size distribution for silver iodide aerosols generated from a hot wire in the experimental apparatus and then aged at room temperature in the aluminum storage vessel for 3 h are shown in Fig. 2. A diffusion battery, a ROYCO optical particle counter (ROYCO Instruments, Inc., Menlo Park, Calif.) and an electrical aerosol analyzer were used to study the evolution of the aerosol particle size distribution as the aerosol aged. Aerosol particles were not visible in the laser beam. Since particles larger than the wavelength of the laser should have been visible, the fraction of particles $\geqslant 0.6$ μm diameter must have been negligible.

It is assumed that the size distribution for silver iodide aerosols aged at subfreezing temperatures was similar to the size distribution for aerosols aged at room temperature and in particular that the largest 1% of these aged aerosol particles was larger than a few tenths of a micrometer in diameter.

The size distribution for the aged lead iodide aerosols was not measured directly, as it is reasonable to assume that the aging process led to a size distribution similar to that shown in Fig. 2 for silver iodide. No un-nucleated lead iodide particles were visible in the laser beam at ice saturation. Thus particles $\geqslant 0.6$ μm diameter were not present in the lead iodide aerosol.

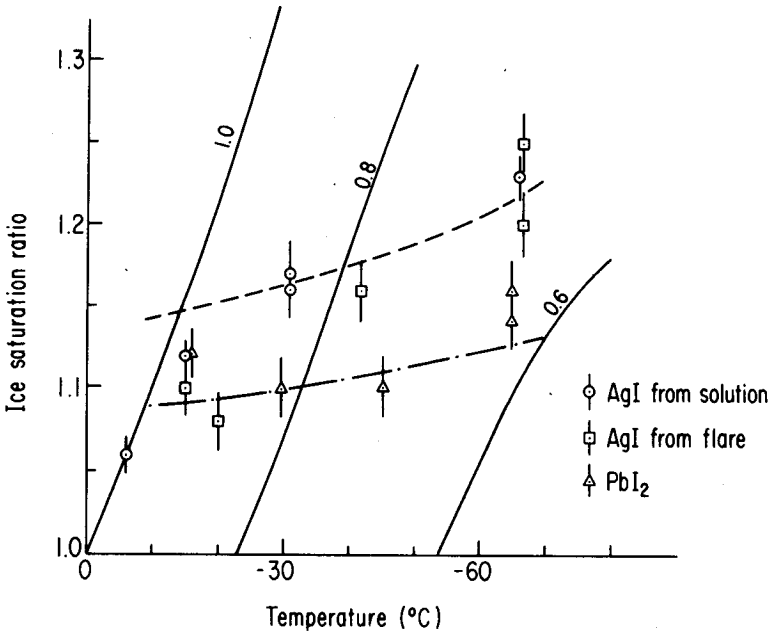

FIG. 3. Observations of the ice saturation ratio required to nucleate 1% of an aged aerosol to ice for various aerosols and at various temperatures. Solid lines sloping upward to the right are lines of constant relative humidity with respect to liquid water. The dashed line is based on Eq. (3) with $S_{T0} = 1.15$ and $T_0 = -15$°C. The dash-dotted line also is based on Eq. (3) with $S_{T0} = 1.1$ and $T_0 = -30$°C.

A threshold ice saturation ratio at which a specified fraction of the aerosol nucleates within a certain time was observed. The fraction and time period were dictated by the idiosyncracies of the experimental set-up and aerosol characteristics. In this study the threshold was chosen as 1% of the aerosol in the laser beam nucleating within a few seconds after the first ice particle appeared. This threshold was easy to estimate by eye, as this typically amounted to a few tens of ice particles in the 0.1 cm^{-3} volume of the beam viewed through the telescope.

It is likely that at this threshold it is the largest particles in an aerosol that begin to nucleate. Theory indicates that, due to the stochastic nature of ice nucleation from the vapor, those particles with the largest surface area are the most likely to nucleate at a given temperature and humidity (see Section 1). The diameter of the aerosol particles nucleating at this threshold, then, was probably of the order of several tenths of a micrometer (see Fig. 2).

4. Results

In Fig. 3 are shown observations of the threshold ice saturation ratio at which 1% of the aged silver iodide and lead iodide aerosol particles nucleated in the first surge of ice particles to appear in the chamber.

For silver iodide, the threshold rises from 1.06 at −6°C to ~1.23 at −67°C. Over this temperature range, the rise is somewhat steeper than is predicted by a calculation based on classical nucleation theory. The prediction of the theory, based on Eq. (3) with $S_{T0} = 1.15$ and $T_0 = -15$°C, is shown by the dashed line in Fig. 3.

At room temperature the silver iodide aerosol was observed to nucleate water droplets in the diffusion chamber at supersaturations with respect to liquid water of less than 0.1%. Since liquid phase saturation was required to nucleate ice at −6°C, it is likely that at this temperature the ice particles observed formed by a condensation-freezing process. At lower temperatures ice must have nucleated either by direct deposition of the ice phase or by a sorption-freezing process since nucleation occurred at humidities less than liquid water saturation.

The lead iodide results in Fig. 3 show a decreasing threshold between −15 and −30°C, with a slightly increasing threshold as the temperature decreased to about −65°C. As shown by the dash-dot line, Eq. (3) can be fit acceptably to the lead iodide results for temperatures near −30°C and below. However, at higher temperatures Eq. (3) cannot predict the observed behavior.

5. Discussion

In Fig. 4 are shown the silver iodide results of this investigation along with those of Mason and van den Heuvel (1959) and Schaller and Fukuta (1979). Similar procedures were used to obtain all of the data shown, although there were minor variations

in technique among the three investigations. Mason and van den Heuvel generated their aerosol from a nichrome wire in a dry nitrogen airflow. Schaller and Fukuta generated their aerosol using a hot, iron plate in room air. The threshold ice supersaturations were determined in thermal gradient diffusion chambers with somewhat different designs. The observations of Mason and van den Heuvel are quite close to those of this investigation (between −6 and −25°C) as far as the overall trend of increasing ice saturation ratio with decreasing temperature when all of their data is considered. The silver iodide aerosol of Schaller and Fukuta behaved somewhat differently. It required substantial liquid water supersaturation for nucleation at temperatures near −6°C and warmer. Below about −15°C it showed a constant threshold ice saturation ratio somewhat smaller than the thresholds observed over the same range of temperatures in the other two investigations.

When the entire range of temperatures and thresholds is taken into account, however, the agreement among the three sets of observations is fair. The size of the silver iodide aerosol particles nucleating at the plotted thresholds was probably nearly the same in all three works, that is, several tenths of a micrometer diameter.

The lead iodide results in Fig. 3 agree nearly exactly with the lead iodide results obtained by Schaller and Fukuta, for a theshold nucleation rate of 1.3% of their aerosol in 1 min, down to about −25°C. (Mason and van den Heuvel did not present lead iodide results.)

It is not clear why, using similar techniques, the results of this investigation and those of Schaller and Fukuta agree so well for lead iodide but differ significantly for silver iodide. It may be that the temperature to which the coated metal surface is heated and the rate at which the volatilized material is quenched in order to produce the silver iodide aerosol are quite critical in determining the deposition ice nucleating characteristics of the resulting aerosol.

Gorbunov *et al.* (1980), have shown that the activity of sub-micron silver iodide particles as freezing nuclei depends on their crystalline structure. Structure also may be important for deposition nucleation. The equilibrium crystalline structure of silver iodide is quite temperature dependent (Fletcher, 1969b). The temperature at which the silver iodide particles condense will depend on the temperature to which the bulk material is heated and how rapidly the volatilized material is cooled. The predominant crystalline structure is not known for the three investigations compared in Fig. 4. Variation in crystalline structure could be responsible for the observed difference in behavior between the results of Schaller and Fukuta and the other two works.

On the other hand, the temperature of formation may not be critical in the case of lead iodide aerosol production.

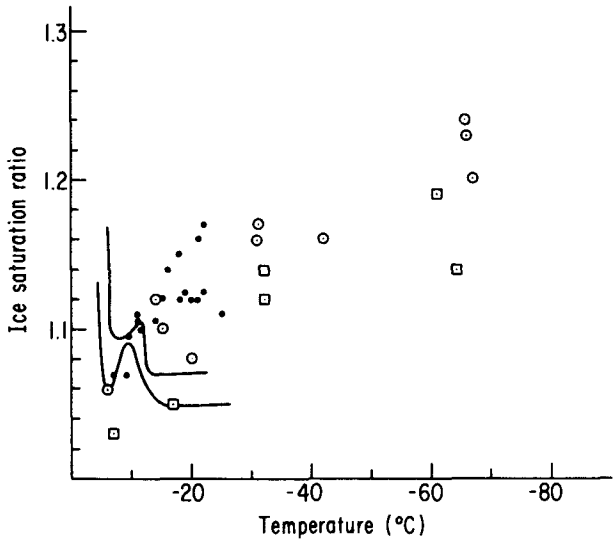

FIG. 4. The threshold ice saturation ratios observed for silver iodide in three similar sets of experiments. The results of Mason and van den Heuvel (1959) are shown as solid dots. The nucleation rate at their stated threshold was not given. The results of Schaller and Kukuta (1979) are shown as solid lines. The upper line is for 6.4% of their aerosol nucleating in 1 min. The lower line is for 1.3% nucleating in 1 min. Our results are shown for two nucleation rates. The circles denote the threshold for 1% of the aerosol nucleating in a few seconds. The squares show the threshold for 0.01% nucleating in a few seconds. Data from the two previous investigations were taken from the published figures.

One notes from Fig. 3 that below about −20°C, 1% of the lead iodide aerosol nucleates at a lower ice saturation ratio than 1% of the silver iodide aerosol. However, our lead iodide thresholds are, as noted, similar to those of Schaller and Fukuta and higher than the silver iodide thresholds reported by them for similar nucleation rates at the same temperatures.

Another possibility is that the disagreement between our silver iodide results and those of Schaller and Fukuta is due to varying types of non-silver iodide contaminants. However, these contaminants did not affect the lead iodide results. In addition, ice nucleation tests also were carried out on the aerosol derived from the clean wire alone, and with lead iodide on platinum wire coils. They show that except for relative humidities > 1.0, the "bare wire" component that may be present in the silver iodide and lead iodide aerosols generated in this study probably does not affect their ice nucleating abilities significantly (Detwiler, 1980).

6. Conclusion

The abilities of submicrometer silver iodide and lead iodide aerosol particles to nucleate ice from the

vapor were observed to depend weakly on temperature in the range −6 to −67°C. The variation in threshold ice saturation ratio was of the order of a few percent or less per 10°C temperature interval.

Silver iodide showed a slowly rising threshold ice saturation ratio for ice nucleation from the vapor as temperature decreased from −6 to −67°C. The lead iodide aerosol tested showed a decreasing threshold between −15 and −30°C and a slowly rising threshold as temperatures decreased from −45°C to near −65°C.

Near and below −30°C these observations agree quite well with a simple calculation using classical nucleation theory. At higher temperatures, apparently, a more detailed treatment of the classical nucleation theory, including parameter variations ignored in the simple treatment, must be employed in order to describe the observed variation of nucleation rate with temperature and humidity.

Since silver and lead iodide aerosols retain their effectiveness as ice forming nuclei at temperatures as low as −67°C, they appear to be good choices as nucleating agents for artificially initiating cirrus cloud formation in regions of clear air that are supersaturated with respect to ice.

Acknowledgments. It is a pleasure to acknowledge the assistance of Mr. Andrew Landor in constructing the experimental apparatus. We also acknowledge the helpful comments of the anonymous referees that helped to improve this presentation. This research was supported by the Atmospheric Research Section, National Science Foundation.

REFERENCES

Detwiler, A., 1980: Clear air seeding. Ph.D. thesis, State University of New York at Albany, 207 pp.

Dufour, L., and R. Defay, 1963: *Thermodynamics of Clouds*. Academic Press, 255 pp.

Fletcher, N. H., 1958: Size effect in heterogeneous nucleation. *J. Chem. Phys.*, **29**, 572–576.

——, 1969a: Active sites and ice crystal nucleation. *J. Atmos. Sci.*, **26**, 1266–1271.

——, 1969b: *The Physics of Rainclouds*. Cambridge University Press, 390 pp.

Gannon, P. T., Sr., 1978: Influence of earth surface and cloud properties on the South Florida sea breeze. NOAA Tech. Rep. ERL 402-NHEML 2, Environmental Research Laboratories, Boulder, 91 pp.

Gray, W. M., and R. W. Jacobson, Jr., 1977: Diurnal variation of deep cumulus convection. *Mon. Wea. Rev.*, **105**, 1171–1188.

Gorbunov, B. Z., N. A. Kakutina and K. R. Loutzenogii, 1980: Studies of silver iodide ice-forming activity: Verification of theory. *J. Appl. Meteor.*, **19**, 71–77.

Heymsfield, A., 1975: Cirrus uncinus generating cells and the evolution of cirriform clouds. Part III: Numerical computations of the growth of the ice phase. *J. Atmos. Sci.*, **32**, 820–830.

Higuchi, K., and N. Fukuta, 1966: Ice in capillaries of solid particles and its effect on their nucleating ability. *J. Atmos. Sci.*, **23**, 187–190.

Jayaweera, K. O. L. F., and T. Ohtake, 1972: Artificial cloud formation in the atmosphere. *Science*, **178**, 504–505.

Lamb, D., and W. D. Scott, 1974: The mechanism of ice crystal growth and habit formation. *J. Atmos. Sci.*, **31**, 570–580.

Letestu, S., Ed., 1966: *International Meteorological Tables*. World Meteorological Organization, No. 188, Geneva.

Mason, B. J., and J. Hallett, 1956: Artificial ice-forming nuclei. *Nature*, **177**, 681–683.

——, and A. P. ven den Heuvel, 1959: The properties and behavior of some artificial ice nuclei. *Proc. Phys. Soc.*, **74**, 744–755.

Nicodemus, M. L., and J. D. McQuigg, 1969: A simulation model for studying possible modification of surface temperature. *J. Atmos. Sci.*, **8**, 199–204.

O'Connor, T. C., and A. F. Roddy, 1966: The production of condensation nuclei by heated wires. *J. Rech. Atmos.*, **2**, 239–244.

——, W. P. F. Sharkey and C. O'Brolchain, 1959: On condensation nuclei produced by heated surfaces. *Pure Appl. Geophys.*, **42**, 109–116.

Pruppacher, H. R., and J. D. Klett, 1978: *Microphysics of Clouds and Precipitation*. D. Reidel, 714 pp.

St. Amand, P., L. A. Burkardt, W. G. Finnegan, L. L. Wilson, S. D. Elliott, Jr. and P. T. Jorgensen, 1970: Pyrotechnic production of nucleants for cloud modification, Part II. Pyrotechnic compounds and delivery systems for freezing nucleants. *J. Wea. Mod.*, **2**, 33–46.

Schaefer, V. J., 1950: The effects produced by seeding supercooled clouds with dry ice and silver iodide. *Centenary Proc. Roy. Meteor. Soc.*, 42–50.

Schaller, R. C., and N. Fukuta, 1979: Ice nucleation by aerosol particles: Experimental studies using a wedge-shaped ice thermal diffusion chamber. *J. Atmos. Sci.*, **36**, 1788–1802.

Vonnegut, B., 1953: Effect of halogens on the production of condensation nuclei by a heated platinum wire. *Science*, **117**, 108–109.

——, and K. Maynard, 1952: Spray-nozzle type silver-iodide smoke generator for airplane use. *Bull. Amer. Meteor. Soc.*, **33**, 420–428.